

The 1997 event in the Crab pulsar revisited

F.Graham Smith, A.G.Lyne, and C.Jordan

Jodrell Bank Centre for Astrophysics

The Alan Turing Building

School of Physics and Astronomy

The University of Manchester

Oxford Rd

Manchester

M13 9PL

UK

8 January 2018

ABSTRACT

A complex event observed in the radio pulses from the Crab pulsar in 1997 included echoes, a dispersive delay, and large changes in intensity. It is shown that these phenomena were due to refraction at the edge of a plasma cloud in the outer region of the Crab Nebula. Several similar events have been observed, although in less detail. It is suggested that the plasma cloud is in the form of filaments with diameter around 3×10^{11} m and electron density of order 10^4 cm⁻³.

Key words: pulsars: general – pulsars: individual: Crab – supernova remnants

1 INTRODUCTION

A dramatic event in the radio pulses received from the Crab Pulsar was observed in October 1997, during routine observations at Green Bank and at Jodrell Bank (Backer et al. 2000; Smith and Lyne 2000). A prominent part of the event was an echo, following both the main pulse and the interpulse, which was attributed to multi-path propagation involving an ionised cloud at a large distance from the pulsar but within the Crab Nebula. As the cloud had crossed the line of sight, a large reduction of intensity was observed, followed by an increase in dispersion measure. Backer et al. describe the event in detail. They propose a model describing the cloud as a prism, attributing the echo to a ray path through the main body of the prism, and the reduction in intensity to a lensing effect as the thick base of the prism crossed the line of sight. Our paper is a revision of this model.

The echo observed on this occasion, and on several others (Lyne et al. 2001), had two components, the first with reducing delay followed after several weeks by a second with increasing delay. It now seems that a more appropriate model would be an essentially symmetric model, involving refraction at the two edges of a cloud rather than within the main body of the cloud. The lensing effect is then the cause of both the delayed ray path and the reduction in intensity. We suggest that the cloud is in the form of a filament, which

crosses the line of sight due to the known proper motion of the pulsar.

A similar analysis has been applied by Crossley et al (2007) to echoes of giant pulses from the Crab pulsar; these echoes had much shorter delays, and were attributed to structure in the inner region of the Crab nebula.

2 THE OBSERVED PHENOMENA

The sequence of events is shown in Figure 1a, which shows the evolution of the pulse profile as observed at 610 MHz during 260 days starting at MJD 50620. Data from the daily monitoring of the Crab pulsar (Lyne et al. 1993) have been used to provide a single high signal-to-noise profile of the pulse each day. Each observation is typically an integration over 12 h, obtained by adding the intensity synchronously at the pulse period (approximately 33 ms). The pulse profile is presented as a grey-scale of intensity on a vertical line in the figure (this is the only available format for this observation). The full rotation period of 33 milliseconds is displayed, and a constant value of slowdown rate $\dot{\nu}$ is used throughout.

The time-scale is adjusted to an ephemeris determined from the pulse arrival times over a period of one month near the middle of the sequence; a vertical track of the pulses in the figure would indicate rotation with normal slowdown.

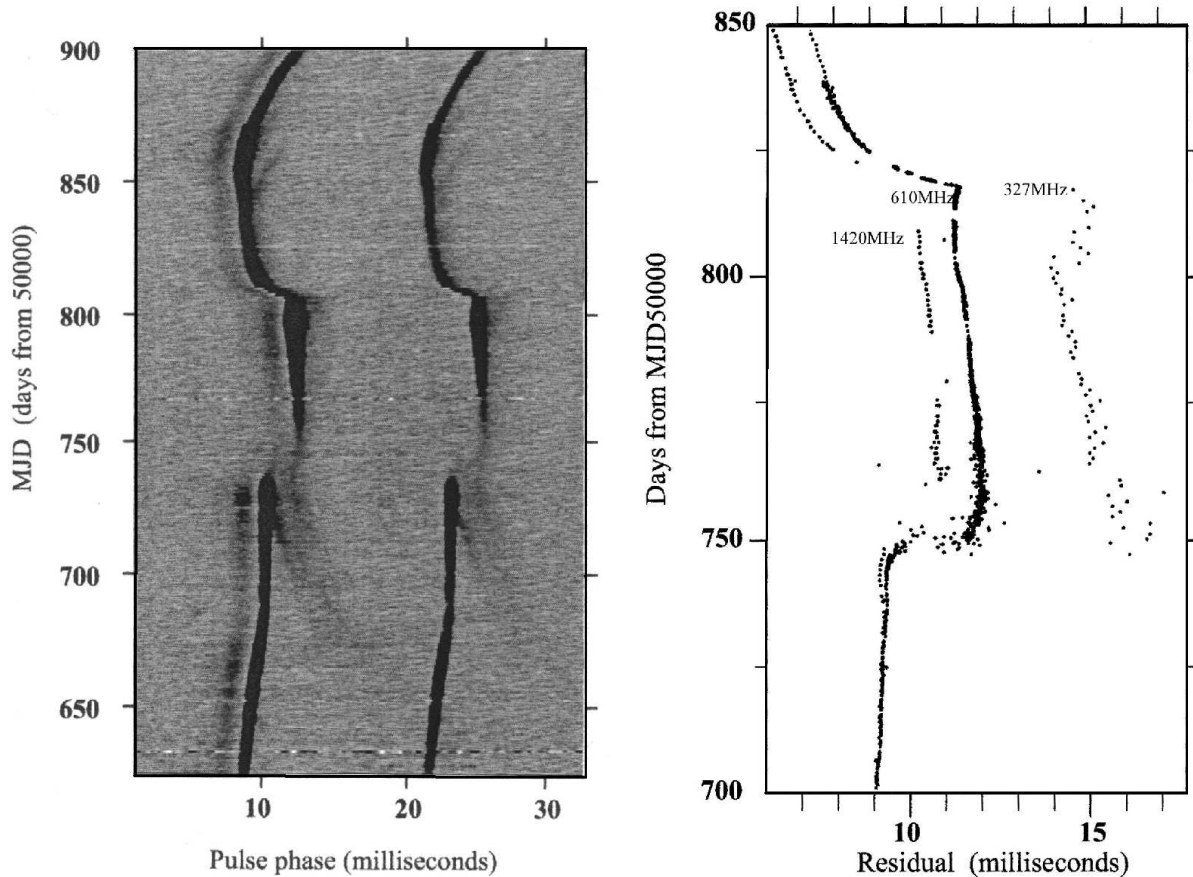


Figure 1. (a) The pulses of the Crab pulsar, recorded at 610MHz by the 13-m radio telescope at Jodrell Bank between 1997 July 17 and December 29 (MJD 50646-50811). Each observation is typically an integration over 12 h, obtained by adding the intensity synchronously at the pulse period (approximately 33 ms). Each horizontal scan shows the three pulse components, which normally trace a vertical line when the pulsar rotation follows a constant slowdown rate. The echoes are seen as diffuse emission following both the main pulse and the interpulse. (b) Pulse arrival times at 1420, 610 and 327 MHz.

The main pulse is preceded by the much weaker precursor and followed 0.013 s later by the interpulse. The behaviour from day 620 to 670 is normal. From day 670 to 720 a faint echo is seen following the two most intense components, with a delay decreasing from about 5 ms to zero at or near day 720. (We have some evidence that a similar echo from the precursor was present, but it is obscured by the more intense main pulse.) The intensity of the echo increases from about 2% to 5% of the normal pulse as the delay decreases.

The intensity of the pulse is known to vary due to interstellar scintillation, but the increase in intensity from day 730 to 740 is unusual and significant. At day 740 all three normal components fade and disappear; they are replaced on day 747 by the same pattern with a delay of 2.3 ms and with intensity increasing until about day 800. On day 812 a glitch occurred; this is a speed-up following the pattern of many previous glitches, and it was presumably unrelated to the other phenomena. The increasing delay after day 860 indicates an increase in slowdown rate, as is normally observed after a glitch in this pulsar. At day 845 an echo is again observed, similar to the earlier echo but with increasing rather than decreasing delay. A similar faint receding echo is also seen at day 800.

Observations were also made at frequencies of 327 MHz (Backer et al 2000) and 1420 MHz (Jodrell Bank). These show similar behaviour, but with different step delays. Figure 1b shows the delays as timing residuals over a period of 150 days which includes all the main events. The pulse arrival times are adjusted to coincide, with zero slope, during the first 30 days. The delay is seen to be dispersive, and previous interpretations have attributed it to propagation through an ionised cloud within the Crab Nebula but at a large distance from the pulsar. It was remarked that the delay did not follow precisely the normal dispersion law, in which the delay should be proportional to ν^{-2} .

The timing observations shown in Figure 1b were used to obtain values of dispersion measure over a period of 330 days. Figure 2a shows the pulse arrival times corrected for dispersion, 2b shows the dispersion measure. Before the event, the dispersion measure was substantially constant at $56.80 \text{ cm}^{-3}\text{pc}$; it increases abruptly to $56.92 \text{ cm}^{-3}\text{pc}$ when the pulse reappears on day 750. It then decreases almost monotonically over the following 250 days to $56.87 \text{ cm}^{-3}\text{pc}$. (Note particularly the steeper fall around day 850, the time of the departing echo.) The value was unaffected by the glitch at day 812. It is this episode of increased disper-

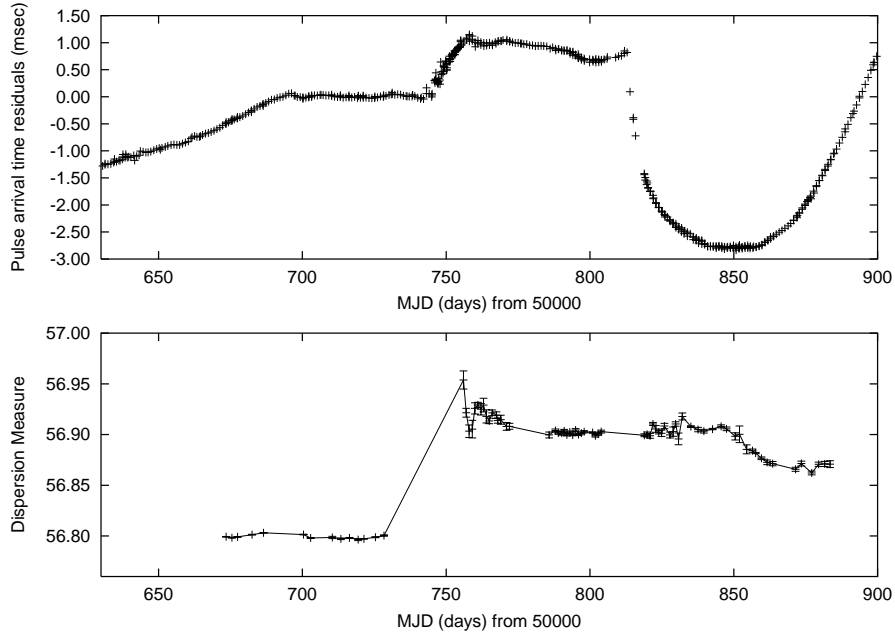


Figure 2. a Pulse arrival times corrected for dispersion. b. The dispersion measure (DM) observed over 330 days.

sion that has naturally been interpreted as the passage of a plasma cloud across the line of sight to the pulsar.

3 THE ECHO DELAY

The echo delay follows the same parabolic path at both 327 MHz and 610 MHz, from a maximum of about 5 milliseconds down to zero; the departing echo observed at day 845 follows a mirror image of the same geometry. This indicates a maximum extra geometrical path $\delta = 1.5 \times 10^3$ km. The echo is evidently due to an object which approaches and moves across the line of sight. In previous analyses, Backer et al. (2000) and Lyne et al. (2001) considered the echo as a specular reflection from the surface of a cloud; we now consider it in terms of refraction within the cloud.

4 A PLASMA LENS

An ionised cloud acts as a diverging lens, since the refractive index is less than one. Clegg, Fey and Lazio (1998) analysed the effect of a plasma lens with Gaussian profile on the apparent brightness of a background source, with particular reference to the effect of a cloud in the interstellar medium on a small diameter extragalactic source; we show that their results are applicable to the echo phenomenon.

Rays from a plane wavefront, passing through any centrally concentrated lens, diverge and avoid a central disc, creating a shadow. Figure 3 shows the shadow behind the tapered edge of a planar disc. Here the wedge diverts rays outward, crossing the undiverted rays and combining with them to increase the intensity. Depending on the shape of

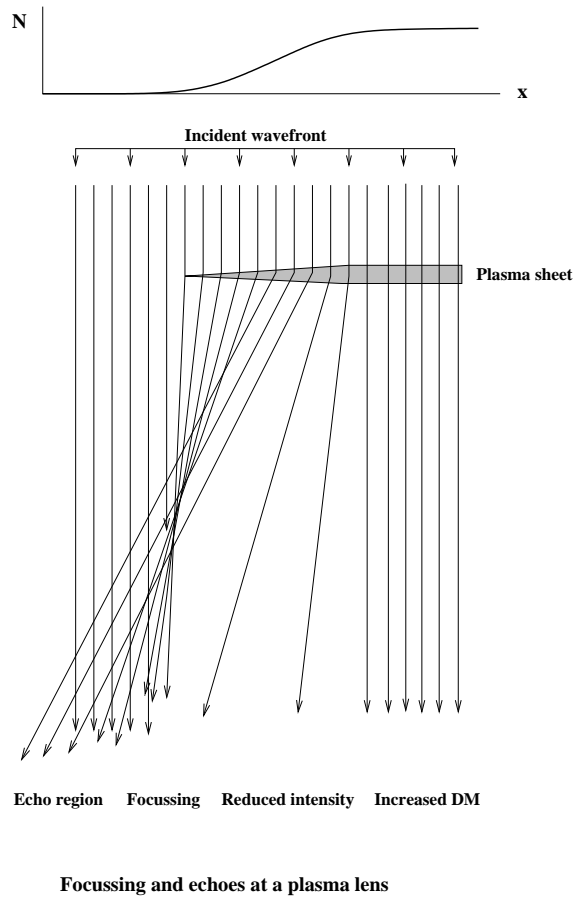


Figure 3. Refraction at the tapered edge of a plasma cloud. The upper curve sketches the variation of total electron content N across the edge of the cloud.

the wedge and the distance of the observer, the rays may combine to form a bright cusp. Further away from the lens the diverging rays give an increased intensity up to a maximum angle which is the maximum refraction angle in the lens. In this region the source is observed as double, with one image formed by rays traversing an extra path. This is the region in which the echoes are observed.

This general picture applies to a cylindrical lens formed by a filament and also to the edges of a plasma sheet. The effect, as seen on a screen, of refraction in a filament is an almost dark line with a bright region on either side, with an extended halo. The dark patch is behind the region of the lens in which there is sufficient gradient to divert the rays out of the line of sight. If the source is pulsed, the halo will show a delay which increases with angular distance.

The observed echoes conform well to this pattern. As the lens approaches the line of sight to the pulsar, the observer is traversing the screen. At the edge of the halo a faint echo is seen at maximum delay. As the delay decreases to zero the observer crosses the cusp, with enhanced intensity. The main pulse then disappears behind the lens (at day 740).

When the main pulse reappears 10 days later it builds up to normal intensity, there is an increase in dispersion measure, and no clear echo appears. This indicates that the lens effect is at the edge of a plasma sheet, in which there is a comparatively low gradient of electron content. A departing echo is observed starting 100 days later, at a time of enhanced intensity, and coinciding with a steep fall in dispersion measure. This is the other edge of the plasma sheet, although it is less well defined as can be seen in Figure 2b.

The scale on the screen can be found from the duration of the event, given only the transverse velocity of the edge across the line of sight. Several examples of echoes have been observed at various times, and all have similar durations and slopes. We suggest that the transverse velocity is almost entirely due to the proper motion of the pulsar, which is observed to be 120 km s^{-1} (Kaplan et al 2008), with no significant contribution from the transverse velocity of the screen itself, and we assume initially that the edge is traversed orthogonally. The shadow region extended for 10 days, i.e. 9×10^5 seconds, giving a scale of 1.0×10^{11} m.

The significant parameters of the lens are its integrated electron content N along a line of sight, and its gradient dN/dx across the line of sight. The overall increase of DM is $0.10 \text{ cm}^{-3} \text{ pc}$, giving a maximum electron content $N_{\text{max}} = 3 \times 10^{21} \text{ m}^{-2}$. Averaged over the shadow region, the lateral gradient dN/dx was $3 \times 10^{10} \text{ m}^{-3}$. Since the echo was observed over a range of angles we assume that the cloud contains structure with larger gradients which gave rise to the echoes at the maximum delay. We explore this by finding the angular deviation corresponding to this averaged overall gradient, and comparing with an independent estimate from the geometry of the observed delays.

The angular deviation in a gradient dN/dx is found from the phase change in traversing a plasma with total

content N . The phase advance is $\lambda r_e N$, where r_e is the classical electron radius $e^2/(m_e c^2) = 2.8 \times 10^{-15}$ m. The angular deviation $\theta = \lambda^2/(2\pi)r_e dN/dx$, where $\lambda = 0.5$ m is the observing wavelength. For the gradient found above the average deviation $\theta_{\text{av}} = 3.2 \times 10^{-6}$ rad.

5 THE DELAY GEOMETRY AND THE LOCATION OF THE PLASMA CLOUD

The echo was first observed 50 days before the delay reduced to zero. At a velocity of 120 km s^{-1} this is a lateral distance $\Delta = 5.2 \times 10^{11}$ m. Using the average deviation angle the distance $R = \Delta/\theta_{\text{av}} = 1.6 \times 10^{17}$ m $\simeq 5$ pc, about 2.5 times the radius of the nebula; a larger local gradient of electron content would give a larger deviation θ and reasonably place the cloud within the nebula.

The echo delay δ is related to R and θ by $\delta = \frac{1}{2c}\theta^2 R$. For the observed maximum delay (5 milliseconds) this yields a maximum deviation angle $\theta_{\text{max}} = 4.3 \times 10^{-6}$, about 1.5 times the angle expected from the average gradient of electron content. The two independent estimates of θ are seen to be reasonably consistent.

The smaller angles of deviation involved as the echo approaches zero delay are derived from parts of the edge with lower gradient. As expected, the echo delay follows a parabolic curve, since it is proportional to Δ^2 .

The distance R derived above places the electron cloud outside the nebula. As noted already, it would be reduced if the cloud contained gradients larger than the average: it would also be reduced if the transverse velocity were reduced below 120 km s^{-1} , as would be the case if the edge were traversed at a non-orthogonal angle. Our analysis is consistent with an electron cloud or filament located within the outer part of the nebula, and with a gradient of electron content given by the calculated average value.

6 THE NON-DISPERSIVE DELAY.

The element of delay, amounting to 1.2 ms, shown in Figure 2 to be independent of frequency, must be related to ray paths in the electron cloud. A lateral gradient of electron content evidently exists in the region traversed by the rays for some days after the event at day 747, and this can account for a geometric delay similar to that observed in the echoes. For this delay to be non-dispersive, however, the refracting region must be localised, so that rays at the three radio frequencies traverse nearly the same geometric path. We suggest that this path is close to the region where there gradient reduces to zero and the profile of electron content becomes flat, as in the idealised model of Figure 3.

7 COMPARABLE EVENTS IN THE CRAB PULSAR

Almost 40 years of recordings exist of the radio pulses from the Crab pulsar. Only three other events comparable to the 1997 event have been recorded, in 1974, 1992 and 1994; echoes were observed in all three, although in the 1974 event, which was the largest, there was insufficient resolution of the echoes to allow a measurement of their delays. It was nevertheless remarked by Lyne and Thorne (1975) that the pulse profiles shown contained discrete components, which we now interpret as echoes; and a re-examination of their published profiles shows that all three components of the pulse (precursor, main, and interpulse) were followed by echoes. The pulse intensity was observed to decrease to near zero in this event, as occurred in 1997. No other comparable event has been found in a close scrutiny of more recent recordings (from 1997 to 2009). The echo delays, and their rates of change, were similar to those in the 1997 event. In our interpretation, this allows us to assume that the edge of the plasma cloud is traversed approximately orthogonally, as in Section 4 above.

Echoes of giant pulses from the Crab pulsar, with delays of 50 - 100 μ s and durations of hours to some days have been observed by Crossley et al (2007), and interpreted using a geometrical analysis similar to ours. These echoes were attributed to a plasma cloud closer to the pulsar, and probably within the diffuse synchrotron nebula. Remarkably the scale of this structure and that of the filament whose effects we have observed are closely similar, despite the different locations in the inner and outer parts of the nebula; both are around one astronomical unit.

Bhat et al (2008) attributed slowly varying scattering of the Crab pulsar observed at 1400 MHz to small-scale filamentary structure in the nebula. Kuzmin et al. (2008) found a close correlation between the incidence of scattering at 100 MHz and changes in dispersion measure of the Crab pulsar, on a time scale of some months. Further observations at Jodrell Bank, and earlier work by Rankin and Counselman (1973) and by Isaacman and Rankin (1977), suggest that these variations are continuous, and not related to the discrete events under discussion. Kuzmin et al. do however suggest that the source of the variable component of the dispersion measure is within the Crab nebula, and that it again has a linear scale of around one astronomical unit.

8 THE NATURE OF THE PLASMA CLOUD

In all three events recorded with sufficient resolution the delay is observed to decrease to zero and subsequently increase in a near parabolic form. This is interpreted as the two edges of a filament crossing the line of sight. In the 1997 event there appears to be a relatively flat profile of electron content across the cloud, but we may interpret the phenomenon generally as a filament with diameter around 3×10^{11} m with a total line-of-sight electron content around 3×10^{21} m⁻². The electron density would then be of order

10^{10} m⁻³, i.e. 10^4 cm⁻³. Direct observation of such filaments by their emission or absorption is a rather remote possibility; milliarcsecond angular resolution would be required, in contrast to the 100 milliarcsecond resolution of the HST observations of filamentary structure in the outer parts of the nebula (Hester et al 1995).

The rarity of these events suggests that the Crab Nebula is only sparsely filled with such filaments. If a typical filament takes several days to cross the line of sight, and the interval between such events is several years, we can envisage a nebula containing only a few thousand such filaments, spaced apart by some hundreds of their diameters and located only in the outer regions. The filaments bear no obvious relation to the well-known visible filaments, and do not contribute significantly to the overall mass of the Nebula.

We thank the referee for helpful suggestions on the presentation of this paper.

REFERENCES

- Backer D. C., Wong T., Valanju J., 2000, ApJ, 543, 740
 Bhat N. D. R., Tingay S. J., Knight H. S., 2008, ApJ, 676, 1200
 Clegg A. W., Fey A. L., Lazio T. J. W., 1998, ApJ, 496, 253
 Crossley J. H., Eilek J. A., Hankins T. H., 2007, in M. Haverkorn & W. M. Goss ed., SINS - Small Ionized and Neutral Structures in the Diffuse Interstellar Medium Vol. 365 of Astronomical Society of the Pacific Conference Series, Echoes of Giant Pulses from the Crab Pulsar. p. 271
 Hester J. J., Mori K., Burrows D., Gallagher J. S., Graham J. R., Halverson M., Kader A., Michel F. C., Scowen P., 2002, ApJ, 577, L49
 Isaacman R., Rankin J. M., 1977, ApJ, 214, 214
 Kaplan D. L., Chatterjee S., Gaensler B. M., Anderson J., 2008, ApJ, 677, 1201
 Kuzmin A., Losovsky B. Y., Jordan C. A., Smith F. G., 2008, A&A, 483, 13
 Lyne A. G., Pritchard R. S., Graham-Smith F., 2001, MNRAS, 321, 67
 Lyne A. G., Thorne D. J., 1975, MNRAS, 172, 97
 Rankin J. M., Counselman C. C., 1973, ApJ, 181, 875
 Smith F. G., Lyne A. G., 2000, in Kramer M., Wex N., Wielebinski R., eds, Pulsar Astronomy – 2000 and Beyond Vol. 202, Gravitational Waves and Neutron Stars. p. 499